



Article

Thermal and Structural Properties of High Density Polyethylene/Carbon Nanotube Nanocomposites: A Comparison Study

Ayat Bozeya ^{1,2,*}, Yahia F. Makableh ^{1,*} , Rund Abu-Zurayk ^{3,4}, Aya Khalaf ⁵ and Abeer Al Bawab ^{2,3,*} 

¹ Institute of Nanotechnology, Jordan University of Science and Technology, Irbid 22110, Jordan; aabouzieh@just.edu.jo

² Chemistry Department, School of Science, The University of Jordan, Amman 11942, Jordan

³ Hamdi Mango Center for Scientific Research, The University of Jordan, Amman 11942, Jordan; r.abuzurayk@ju.edu.jo

⁴ Nanotechnology Center, The University of Jordan, Amman 11942, Jordan

⁵ Department of Basic Sciences, Faculty of Arts and Sciences, Al-Ahliyya Amman University, P.O. Box 108, Amman 19328, Jordan; a.khaled@ammanu.edu.jo

* Correspondence: yfmakableh@just.edu.jo (Y.F.M.); drabeer@ju.edu.jo (A.A.B.); Tel.: +962-7-7568-6460 (Y.F.M.); +962-7-9666-1601 (A.A.B.)

Abstract: The effects of functionalization of carbon nanotubes on the properties of nanocomposite sheets prepared from high-density polyethylene (HDPE) and carbon nanotubes (CNTs) were investigated. Carbon nanotubes were first oxidized, followed by amine group functionalization. The Fourier transform-infrared (FTIR) spectroscopy results confirm the presence of oxygenated and amide groups at the surface of the CNTs after each treatment. The HDPE/CNT nanocomposite sheets were prepared using a melt compounding method. Six types of CNTs were used; pristine Single-walled Carbon nanotubes (SWCNT) and pristine Multi-walled Carbon nanotubes (MWCNT), oxidized (O-SWCNT and O-MWCNT) and amide (Amide-SWCNT and Amide-MWCNT). All prepared nanocomposite sheets were characterized using Thermal gravimetric analysis (TGA), Differential scanning calorimetry (DSC), X-ray diffraction (XRD) and scanning electronic microscope (SEM). TGA results measured increased thermal stability of the polymer with the addition of CNTs, O-MWCNT showed the best enhancement. XRD measurements confirmed that the addition of CNTs did not change the crystal structure of the polymer, although the crystallinity was decreased. The maximum crystallinity decrease resulted from O-SWNTs addition to the polymer matrix. SEM imaging showed that oxidized and functionalized CNTs have more even dispersion in the polymer matrix compared with pristine CNTs.

Keywords: HDPE Polymer; SWCNT; MWCNT; nanocomposites; melt compounding; O-CNTs; amide-CNTs



Citation: Bozeya, A.; Makableh, Y.F.; Abu-Zurayk, R.; Khalaf, A.; Bawab, A.A. Thermal and Structural Properties of High Density Polyethylene/Carbon Nanotube Nanocomposites: A Comparison Study. *Chemosensors* **2021**, *9*, 136. <https://doi.org/10.3390/chemosensors9060136>

Academic Editor: Filippo Giubileo

Received: 16 April 2021

Accepted: 7 June 2021

Published: 11 June 2021

Publisher's Note: MDPI stays neutral with regard to jurisdictional claims in published maps and institutional affiliations.



Copyright: © 2021 by the authors. Licensee MDPI, Basel, Switzerland. This article is an open access article distributed under the terms and conditions of the Creative Commons Attribution (CC BY) license (<https://creativecommons.org/licenses/by/4.0/>).

1. Introduction

High-density polyethylene (HDPE) polymer is routinely used for a wide variety of high-end applications such as household plastic products, distribution pipes, heavy duty bags, agriculture packaging, toys, and many others [1–3]. However, industrial application of HDPE is limited by its low strength (Tensile strength, yield at 23 °C (23.0–29.5 MPa), Break at 23 °C (30.5–33 MPa) [3,4]. The introduction of inorganic nanomaterials, as reinforcing materials into polymer systems, resulted in nanocomposite (polymer nanostructural materials), thus exhibiting multifunctional, high performance polymer characteristics beyond that of the traditional polymer [5]. The reinforcing material (nano material) can be particles, sheets, fibers, or nanotubes. The large surface area of reinforcement material means that a relatively small amount of nano-scale reinforcement material can have an observable effect on the macro scale properties of the polymer nanocomposite systems [6–10].

Carbon nanotubes (CNTs) have drawn significant interest from the scientific community due to their unique mechanical, electrical and thermal conductivity properties which have now been the focus of countless fundamental studies from both theoretical [11,12] and experimental perspectives [8–13]. These studies have found that CNTs have interesting reinforcement properties when used incorporated in the polymer matrix while strongly influencing the material properties of polymer nanocomposites [10,11]. The major challenges in the practical implementation of CNTs for industrial applications are enhancing their dispersibility and chemical compatibility in other materials systems [11,13]. A potential solution for this is the use of surface treatments, including chemical oxidation of CNTs. Several methods of chemical oxidation of CNTs have been reported in the literature: wet chemical oxidation (using acids) [14–19], plasma treatments oxidation [20,21], ozone and hydroxyl radicals [22], ionizing environment [23], and synthetic organic chemistry [24]. The most common method is wet chemical oxidation using different oxidizing acids (H_2SO_4 , HNO_3 , or $\text{H}_2\text{SO}_4/\text{HNO}_3$ solution) or strong oxidants (O_3) [25] due to the ease of implementation in a laboratory and industry setting. Chemical oxidation with acids damages the graphite-like structure, generates chemically active defects, and attaches various chemical (oxygenated) groups. The diversity and abundance of attached groups depend on the oxidation protocol and type of acid used [8,26,27]. Further functionalization of the oxidized CNTs is achieved by converting the oxygenated surface groups to other functional groups such as esters or amides by direct coupling between an organic amine or ester and the oxygenated (carboxylic acid) groups previously formed on the CNT surface [28,29]. The primary obstacle for functionalizing the oxidized CNTs (O-CNTs) is selecting an ideal organic molecule, which must be able to provide both efficient surface bonding with CNTs and reactivity towards the polymer matrix in the polymer nanocomposite [30].

A wide variety of preparation methods have been used to improve dispersion of CNTs in the HDPE polymer matrix [31–33], such as melt processing, solution casting, in situ polymerization, and mechanical agitation of molten polymer followed by compression casting and spin casting [34–39]. The melt compounding method is among the most widely used due to its advantages of large scalability and high controllability [32,40–42]. This method involves melting of the polymer to form a viscous liquid, then introducing the reinforcing additives to the polymer feed [43]. Many different HDPE/CNT nanocomposites have been successfully prepared using this method. Tang et al. (2003) was the first group to combine HDPE and CNT to form a HDPE/CNT composite using as-synthesized multi-wall CNTs (MWCNTs) without any further modification [31]. Kanagaraj et al. (2007) synthesized HDPE/MWCNT composites using the injection molding technique, in which the HDPE polymer was melted at 200 °C in the plasticized unit of the injection moulding to enhance the mixing of the polymer with the CNTs, then the mixture was injected into a tensile specimen. In this process, MWCNTs were first chemically treated with acids to achieve better interfacial bonding between MWCNT and the HDPE polymer while enhancing the load transfer properties [44].

While most HDPE/CNT studies focus on the mechanical or electrical properties [45–49], a few studies have shown that the addition of CNTs to the HDPE polymer matrix increase the crystallinity or thermal stability of the polymer. For instance, additions of 1% pristine CNTs (P-CNTs) to the HDPE polymer matrix using mechanical agitation increased the crystallinity of the polymer from 53.6% to 56.6% [45]. Furthermore, Salehi et al. (2019) reported that additions of 5% functionalized MWCNT with steric acid to the HDPE polymer matrix increased the onset crystallization temperature and crystallinity by 2.89 °C and 1.8%, respectively [46]. In another study, adding 1% MWCNT to HDPE increased the melting temperature by 2 °C and decreased the heat of crystallization by 16%, indicating imperfect crystallization of the HDPE matrix upon addition of MWCNT [50].

Even though HDPE/single-wall CNTs (SWCNTs) and HDPE/MWCNTs composites have been extensively investigated, the effects of different CNT sources (i.e., functionalized CNTs, P-CNTs, O-CNTs, SWCNT, and WMCNT) on the thermal and structural properties of HDPE/CNT composites has not been well studied. Examining thermal and structural

changes of HDPE/CNT nanocomposites is crucial for synthesis, especially towards tuning mechanical properties. This investigation compares functionalized, oxidized, and pristine CNTs on the thermal and structural properties of HDPE/CNT nanocomposites prepared by melt compounding. Different types of CNTs were used (pristine, oxidized, and amide SWCNTs and MWCNTs). The nanocomposites were characterized using TGA, DSC, FTIR, XRD, and SEM. By combining these characterizations, we have obtained a detailed picture of the morphology and thermal properties of various HDPE/CNT nanocomposites, a crucial step towards the implementation of these materials for lightweight, high strength applications.

2. Materials and Methods

2.1. Materials

SWCNT (1.3–2.3 nm in diameter, >70% carbon as SWCNT) (Sigma Aldrich, Bangalore, India), MWCNT (outer diameter (O.D.) \times (inner diameter (I.D.) \times length (L) (10 nm \pm 1 nm) \times (4.5 nm \pm 0.5 nm) \times (3–6 μ m), $d = 2.1$ g/mL, 70–80% carbon content) (Sigma Aldrich, Darmstadt, Germany), oxalyl chloride ($\geq 99\%$) (Sigma Aldrich, Beijing, China), sulfuric acid (98 wt.%) (Sigma Aldrich, Germany). N, N-dimethyl formamide, ethylenediamine anhydrous (99.0%) (TEDIA, Fairfield, OH, USA), tetrahydrofuran anhydrous stabilized (99.8%) (TEDIA, USA), ethanol anhydrous (91%) (TEDIA, USA). Nitric acid (70 wt.%) (SDFCL (s d fine-chem limited), Maharashtra, India). High density polyethylene pellets ($d = 0.954$ g/cm³, Melt index (190 °C/2.16 kg): 0.35 g/10 min) (Sabic, Riyadh, Saudi Arabia), these materials were used as received without any further purification.

2.2. Methodology

2.2.1. Oxidation and Amide Functionalization of CNTs

P-CNT (SWCNTs or MWCNTs) were oxidized by dispersing the CNTs in a mixture of sulfuric (98 wt.%) and nitric acid (70 wt.%) with volume ratios of (1:3 sulfuric: nitric). The resultant suspension was refluxed overnight at 70 °C. The dispersion was then diluted with distilled water, filtered through a cellulose membrane (0.45 μ m pore diameter), and repeatedly washed with distilled water until reaching pH 7. Finally, the CNTs were peeled from the membrane and dried in an oven at 50 °C for 24 h.

The synthesized oxidized CNT (O-CNT; O-SWCNT or O-MWCNT) were dispersed in N, n-dimethyl formamide (DMF) in a sonication bath until a fully dispersed suspension was formed. This dispersion was transferred to an ice bath with a magnetic stirrer, and oxalyl chloride was added under nitrogen. These conditions were maintained for two hours, followed by two hours of stirring at room temperature. After this step, stirring overnight at 70 °C was performed to remove the excess oxalyl chloride. Afterwards, ethylene diamine was added, and the suspension was stirred at 95 °C for three days. After cooling to room temperature, the suspension was filtered through a cellulose membrane (0.45 μ m pore diameter) and subsequently washed with DMF, ethanol, and tetrahydrofuran. The synthesized amide CNT (amide-CNT; amide-SWCNT or amide-MWCNT) were peeled off from the membrane and dried in an oven at 50 °C for 24 h.

2.2.2. Preparation of HDPE/CNTs Nanocomposite Sheets

Nanocomposite sheets were prepared by using a melt compounding method. First, CNTs were dispersed in water using a sonication bath for one hour, then mixed with HDPE pellets. After that, the mixture was heated and continuously stirred using a magnetic stirrer to achieve a uniform coating of CNTs on the HDPE pellets. Once the water was evaporated, the CNT-coated HDPE pellets were dried in an oven at 100 °C for 24 h. to evaporate any extra moisture.

The prepared CNT-coated HDPE pellets were extruded using a DSE-20B co-rotating twin screw extruder (D = 20 mm, L: D = 40). The barrel temperature, from the entrance to the exit (zone I, zone II, zone III, zone IV, zone V, die-head and melt temperature) were 154, 164, 175, 175, 160, 160, 160 °C, respectively. The feeding rate was fixed at 7 g/min. The

extruded HDPE/CNTs nanocomposites strip was cooled to room temperature, then cut to small pieces for compression molding using a CARVER bench top press. The hot press plates were heated to 195 °C and manually compressed to a pressure of ~1 metric ton for 20 min.

Seven sheets were produced by using six types of CNTs: P-SWCNT, P-MWCNT, O-SWCNT, O-MWCNT, amide-SWCNT, and amide-MWCNT. All prepared nanocomposite sheets contained 1 wt.% of CNTs. In addition, pure HDPE was prepared and used as a reference. The seven samples are named M1–M7, as shown in Table 1.

Table 1. Summary of the prepared HDPE/CNTs nanocomposite sheets.

Sample Name	CNTs Type	HDPE/CNTs Nanocomposite Sheet
M1	Reference sample	HDPE
M2	Pristine-SWCNT	HDPE/P-SWCNT
M3	Oxidized-SWCNT	HDPE/O-SWCNT
M4	Amide-SWCNT	HDPE/Amide-SWCNT
M5	Pristine-MWCNT	HDPE/P-MWCNT
M6	Oxidized-MWCNT	HDPE/O-MWCNT
M7	Amide-MWCNT	HDPE/Amide-MWCNT

2.3. Characterization

Fourier transform-infrared spectroscopy (FTIR) was performed using a Thermo Nicolet NEXUS 670 (Gaithersburg, MD, USA), using 32 scans over the range 4000–400 cm^{-1} with 4.0 cm^{-1} resolution. Samples were characterized using KBr. Thermal gravimetric analysis (TGA) was performed using a STA 409 PG/PC TGA NETZSCH instrument (NETZSCH-Geratebau GmbH, WittelsbacherstraBe, Berlin, Germany). Samples were analyzed in Al_2O_3 pans at a heating rate of 10 °C/min from 25 °C to 800 °C in a nitrogen atmosphere. Sample masses ranged from 4–5 mg. Differential scanning calorimetry (DSC) was performed using a DSC 204 F1 Phoenix NETZSCH instrument (NETZSCH-Geratebau GmbH, WittelsbacherstraBe, Germany). Five milligrams of the sample were encapsulated in standard aluminum pans. The samples were heated from 25 °C to 220 °C at a rate of 10 °C/min, then kept at 220 °C for three min, followed by cooling to 25 °C at 10 °C/min under nitrogen atmosphere. X-ray diffraction (XRD) patterns were performed at 2 θ scanning range of 2–60° with a step size of 0.02° using a 7000 Shimadzu (2 kW) model X-ray spectrophotometer instrument (Shimadzu, Kyoto, Japan) with a nickel filtered copper radiation ($\text{CuK}\alpha$) with $\lambda = 1.5456 \text{ \AA}$. Sample morphology was investigated using scanning electronic microscope (SEM), the analysis was performed using a SEM QUANTA FEG 450 instruments, (FEI, Eindhoven, Netherland). Samples were placed on aluminum stubs and sputtered with gold (5 nm thickness).

3. Results and Discussion

FTIR analysis was used to qualitatively detect the presence of oxygenated functional groups at the O-CNTs surface and amide functional groups at the amide-CNTs surface. Figure 1 shows the FTIR spectra of the treated (oxidized and amide) and untreated (pristine) CNTs.

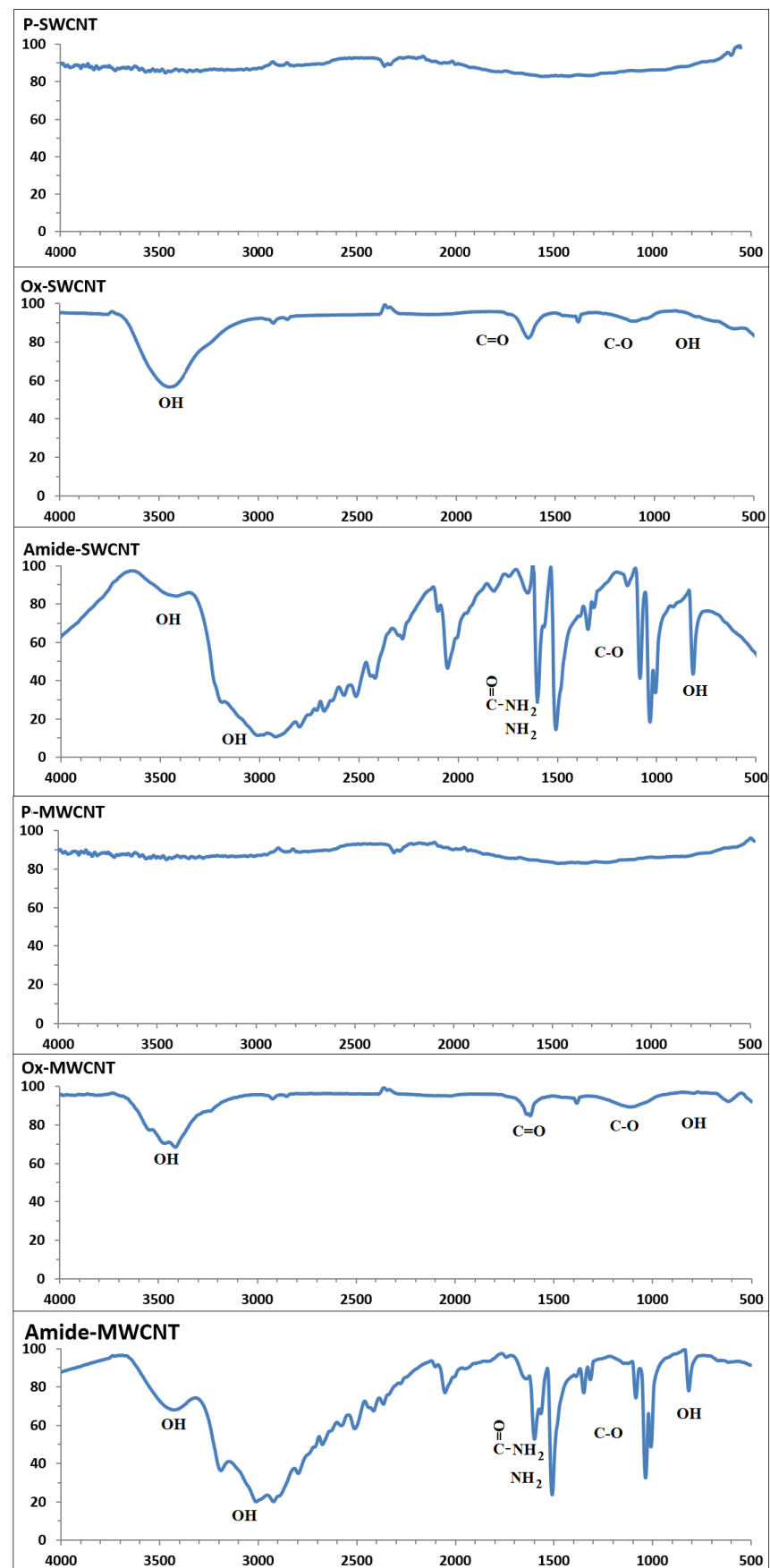


Figure 1. FTIR spectra for the pristine, oxidized and amide CNTs.

The CNTs were functionalized using different functional groups (hydroxyl (OH), carbonyl (C=O), ether (C-O), and amine (NH₂)). A distinct 1730 cm⁻¹ peak, 3429 cm⁻¹ broad band, and 1380–1430 cm⁻¹ are attributed to the presence of carbonyl, OH-stretching vibration, and OH bending vibrations, respectively. In the amide spectrum, a new, strong broad band at 3200–3500 cm⁻¹ can be assigned to the N-H, NH₂, and OH stretching modes. The carbonyl band in the amide spectrum is shifted to 1600 cm⁻¹ compared with 1700 cm⁻¹ in the oxidized spectrum because of amide linkage formation. The other peak at approximately 1510 cm⁻¹ is due to the NH₂ scissoring mode. These observations are strong evidence for the introduction of a functional group on the CNTs [45,51,52].

Digital images, taken by a digital camera of the prepared nanocomposite sheets are shown in Figure 2. All these nanocomposite sheets are appearing nearly identical as black color sheets due to the presence of the CNTs.

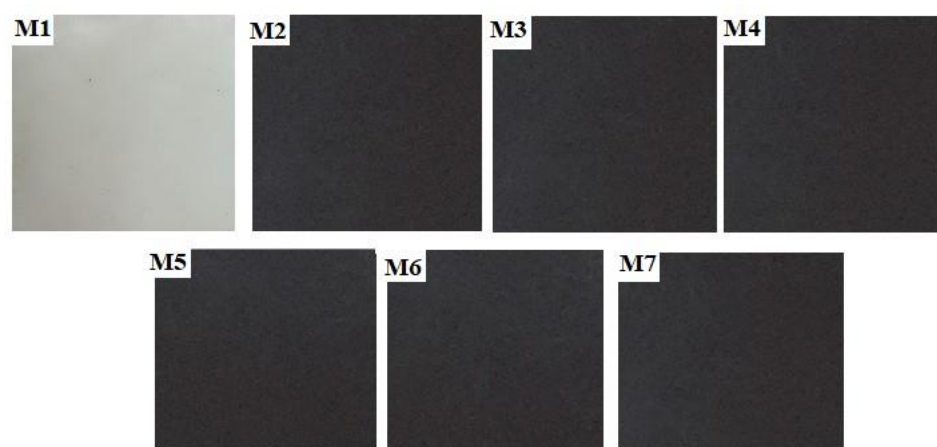


Figure 2. Digital images of the prepared nanocomposites sheets of HDPE/CNTs samples (M1–M7).

The TGA and the DTG degradation graphs for the prepared sheets are shown in Figures 3 and 4, respectively. The onset decomposition temperature (T_{95}); the temperature at which 5% weight loss of the sample occurs, the degradation temperature (T_{on}); the first derivative of the TG curve, and the residue content (Summarized in Table 2), were taken to describe the thermal stability of the prepared nanocomposites. The T_{95} and T_{on} for all nanocomposites sheets were higher than that of pure HDPE, indicating an improvement in the nanocomposites' thermal stability by 4–12 °C and 2.8–6.7 °C for T_{95} and T_{on} , respectively. The T_{95} for the pure HDPE sheet was approximately 444 °C. This thermal stability improvement can be attributed to the addition of CNTs, as they exfoliate between the polymer chains and retard their mobility, making them more thermally stable with a higher T_{95} [44,53]. The residue content was in the range 1.13–1.77% which is acceptable values and close to the added % of the CNT (1%).

Table 2. Summary of the TGA results of the prepared HDPE/CNTs nanocomposite sheets under air atmosphere, at a heating rate of 10 °C/min.

Sample Name	T_{95} (°C)	T_{on} (°C) First Derivative T	Residue Content (%)
M1	444	459.9	1.61
M2	448	463.6	1.77
M3	448	465.2	1.29
M4	448	462.7	1.55
M5	451	464.8	1.13
M6	456	466.8	1.21
M7	453	466.5	1.21

In most cases the increase in the T_{95} and T_{on} , is an indication of the improvement of the thermal stability. Ferreira et al. reported some enhancement of the thermal stability of HDPE polymer when the T_{95} increased in the range of 2.8–13.1 °C, after addition of CNT (2.8 °C), carboxylic acid functionalized CNT (9.5 °C) and Dodecylamine functionalized CNT (13.1 °C) [37]. Additions of any type of MWCNT resulted in a greater increase in the T_{95} compared with additions of any type of SWCNTs. This can be attributed to the size difference between the SWCNT (smallest size 1.3–2.3 nm) and MWCNT (largest size 10 nm \pm 1 nm). The larger MWCNT limits the diffusion of volatile decomposition products, improving the thermal stability of the nanocomposite. As described by Kodjie et al. (2006), the thermal degradation of HDPE occurs by random chain scission to form radicals of alkyl and alkyl peroxy that are susceptible to inhibition reagents capable of trapping the radicals [54]. Shi et al. reported that the structural difference between the composite prepared with modified CNT and unmodified CNT showed different thermal stability [55]. The best thermal enhancement was produced by O-MWCNT. This might hold the key for radical scavenging and, therefore, more thermal stability. As the O-CNTs have the highest electron affinities compared with P-CNTs and Amide-CNTs, and O-CNTs have the highest ability to hydrogen bond with the HDPE molecular chain. Although amide-CNTs could form hydrogen bonds with HDPE molecular chains as well, their size difference compared with O-CNTs limited their positive impact on thermal stability [53,56].

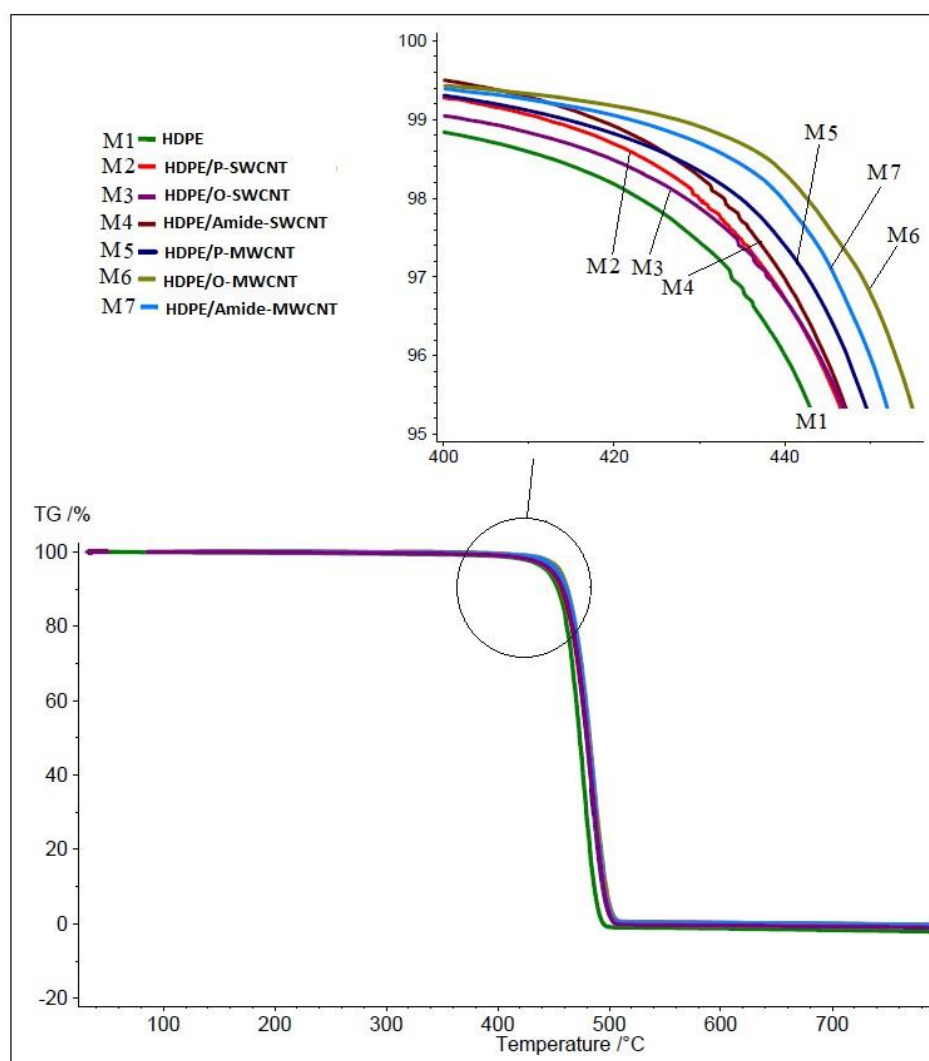


Figure 3. TGA degradation graphs for the nanocomposite sheets M1–M7 performed with heating rate of 10 °C/min from 25 °C to 800 °C in nitrogen atmosphere.

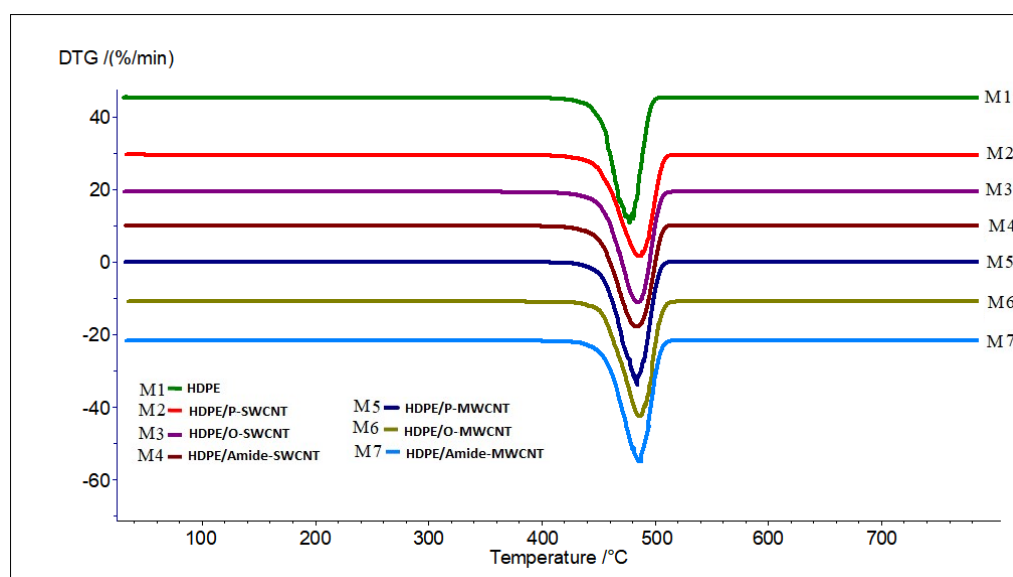


Figure 4. DTG degradation graphs for the nanocomposite sheets M1–M7 performed with heating rate of 10 °C/min from 25 °C to 800 °C in nitrogen atmosphere.

DSC was used to measure the melting and crystallization behavior of the prepared sheets. The heating and cooling thermograms are presented in Figures 5 and 6, respectively. Table 3 lists the DSC data (the peak melting temperature T_m , heat of fusion and the percent crystallinity for all the prepared nanocomposites sheets.

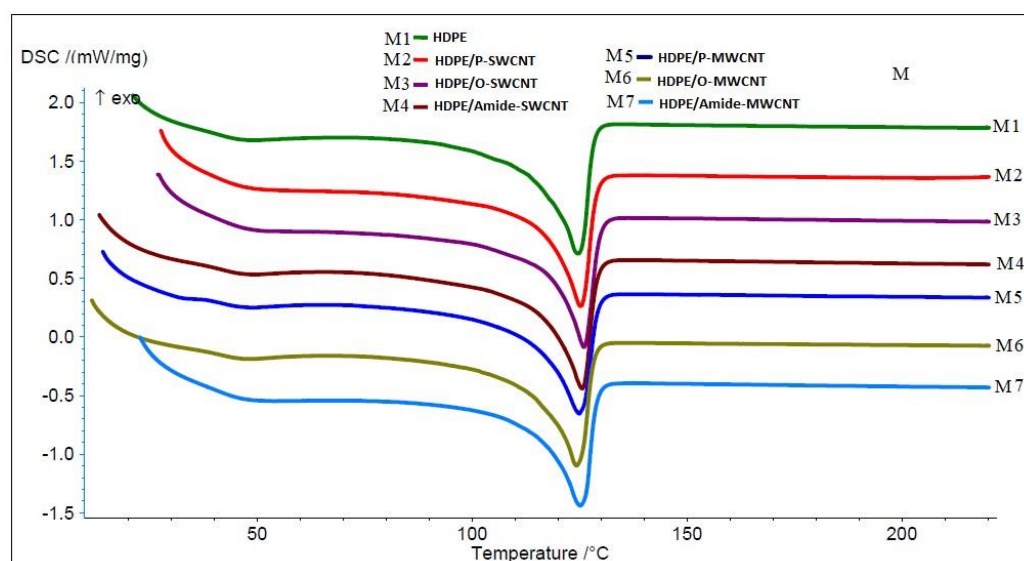


Figure 5. The DSC heating thermograms for the nanocomposite sheets M1–M7 measured with heating rate of 10 °C/min from 25 °C to 220 °C, under nitrogen atmosphere.

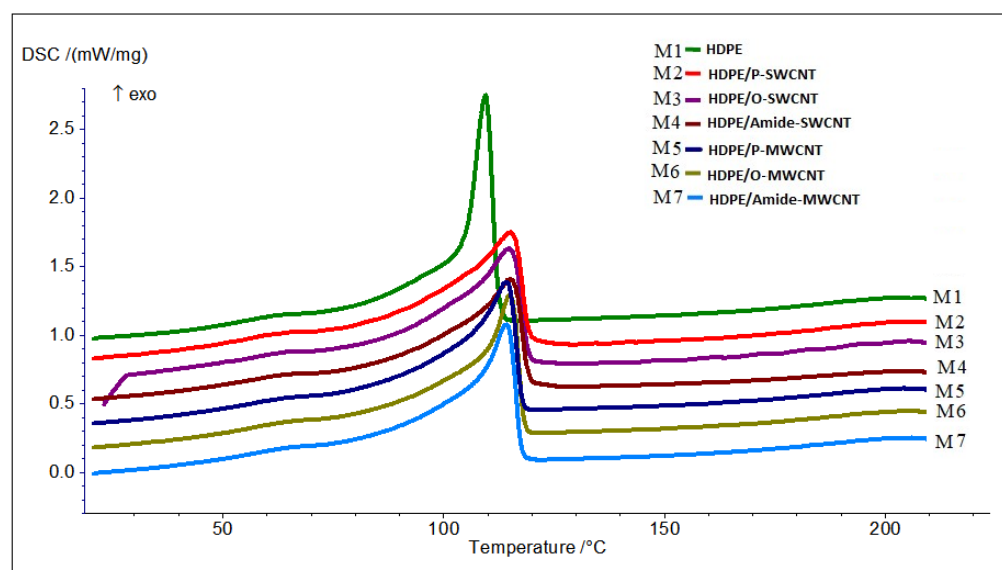


Figure 6. The DSC cooling thermograms for the nanocomposite sheets M1–M7 measured with heating rate of 10 °C/ min from 25 °C to 220 °C under nitrogen atmosphere.

Table 3. Summary of the DSC results of the prepared HDPE/CNTs nanocomposite sheets under nitrogen atmosphere, at a heating rate of 10 °C/min. 25 °C to 220 °C.

Sample Name	T _m (°C)	T _c (°C)	ΔH _m (J/g)	%Crystallinity *
M1	124.8	109.6	90	31
M2	125.4	115.3	87	30
M3	126.1	115.1	86	30
M4	125.7	115.4	82	28
M5	125.0	114.4	84	28
M6	124.3	115.1	89	31
M7	125.3	114.4	83	29

* The crystallinity was calculated based on the heat of fusion of pure HDPE as 293.6 J/g (Kodjie et al., 2006) with 100% crystallinity, and the mass fraction of the HDPE polymer.

The CNTs have negligible effects on the melting temperature (T_m) of all prepared nanocomposites sheets with T_m changes being maintained within the range of (1–2 °C). The crystallization temperature (T_c) of the nanocomposites was shifted to a higher temperature in the range of (4.8–5.8 °C). The increase in crystallization temperature indicates that there is an interaction between the CNT and the HDPE, while the CNTs act as nucleating agents as reported previously in Ferreira et al. study [37]. The crystallinity was calculated based on heat of fusion for pure HDPE ($\Delta H_m = 293.6$ J/g) [54]. The addition of CNTs minimally affected the crystallinity of the polymer matrix, as the decrease in crystallinity was limited to 1–3%. This is expected since melt compounding methods expose the polymer to much higher shear forces that break down CNTs to a small enough size to limit crystal growth. The decrease in crystallinity by additions of MWCNTs was larger than the decrease measured by SWCNT additions. This can be attributed to the fact that the aspect ratio of the SWCNTs is higher than that of MWCNTs. As a result, MWCNTs deform the molecular chain orientation of the polymer, decreasing intermolecular interactions and subsequently decreasing the crystallinity [57,58]. This also causes SWCNTs to be more evenly dispersed in the polymer matrix, resulting in a higher impact on the polymer properties. Similar results were obtained by other researchers [59,60], although some reports measure increased crystallinity value by CNT additions [45,46].

SEM imaging for the prepared nanocomposites sheets is shown in Figure 7. The prepared nanocomposites sheets were characterized using SEM to evaluate the embedding of CNTs in the HDPE matrix. As shown in Figure 7, the CNTs embedded in the polymer

matrix appear evenly dispersed between the polymer chains and enhance the connection between the polymer chains. This is expected due to the high force CNTs are exposed to during extrusion, which works to effectively disperse CNTs within the polymeric matrix [61].

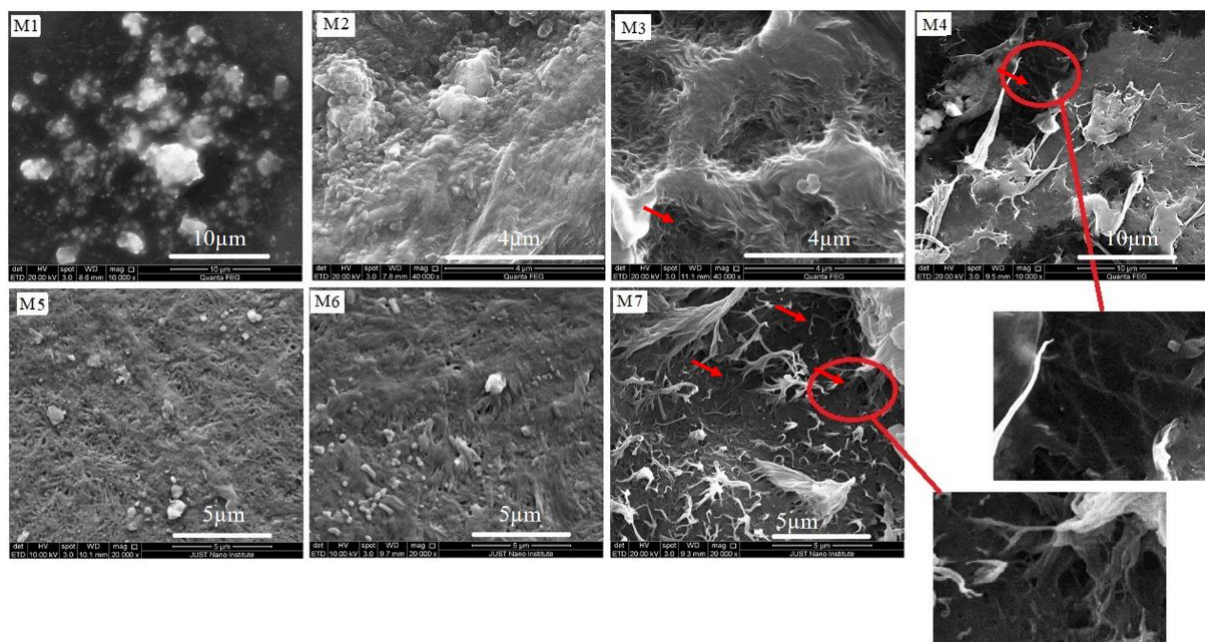


Figure 7. Scanning electron microscope images of (M1–M7) showing the embedding of CNTs in the polymeric matrix.

The embedding of CNTs in the polymer matrix increased in the following order: amide-CNTs > O-CNTs > P-CNTs. The increase in embedding may be related to the presence of the functional groups (oxygenated and amide), which are confirmed by the FTIR analysis. SWCNTs show greater embedding compared with MWCNT, which can be related to the difference in the aspect ratios; the higher aspect ratio of SWCNTs provides easier embedding in the polymer matrix [46].

Prepared sheets were characterized using XRD to qualify the effect CNT additions on the crystal structure of the polymer matrix. Figure 8 shows the measured XRD patterns for all prepared sheets. Pure HDPE mainly exhibits a strong reflection peak at $2\theta = 21^\circ$, followed by a less intensive peak at $2\theta = 23^\circ$, which correspond to the typical orthorhombic unit cell structure of (110) and (200) reflection planes, respectively. Additionally, these 2θ values are in good agreement with the reported values of polyethylene. Additionally, there are three weak peaks at $2\theta = 30^\circ$, 36° , and 39° of the reflection planes (210), (020), and (011) were distinguished, respectively [62,63]. Figure 8 shows the normalized X-ray diffraction measurements performed on the prepared sheets M1–M7 at 2θ scanning range of $2\text{--}60^\circ$ with a step size of 0.02° .

The crystallinity and lattice constants (a , b , and c , were calculated based on an orthorhombic structure) are summarized in Table 4. These were calculated using Origin Pro software by measuring the area under the peaks (crystal) divided by the total peak area (crystal + amorphous), grain size (using Scherrer's equation [64]).

The crystal size was calculated using Scherrer's equation.

$$D = \frac{K\lambda}{\beta \cos\theta}$$

where D : the crystallite size(\AA)

K : Scherrer shape factor

λ : Wavelength

β : The full-width-half-maximum (FWHM) value of the peak in radians

θ : The Bragg angle of the (hkl) reflection plane.

The space between atomic lattices was calculated using Bragg's equation.

$$[2d\sin\theta = n\lambda]$$

where θ : the angle of diffraction

d : the space between atomic lattices

n : positive integer

The lattice constant was calculated based on an orthorhombic structure as follows:

$$\frac{1}{d^2} = \frac{h^2}{a^2} + \frac{k^2}{b^2} + \frac{l^2}{c^2}.$$

where d : the space between atomic lattices

(h, k, l) : The orientation of the orthorhombic plane

$(a, b, \text{ and } c)$: The lattice constant.

The (200) plane was used to calculate the value of a , (020) plane was used to calculate the value of b , and the (011) plane was used to calculate the value of d [64].

Table 4. Crystallinity, Crystal size and lattice constant (a , b , and c) for the HDPE/CNTs nanocomposite sheets.

Sample	% Crystallinity	Grain Size (Å)	Lattice Constant (Å)
M1	63.4	155.5	$a = 7.533, b = 5.000, c = 2.542$
M2	67.2	139.0	$a = 7.431, b = 4.934, c = 2.477$
M3	68.0	152.4	$a = 7.517, b = 4.988, c = 2.493$
M4	65.4	164.9	$a = 7.552, b = 5.018, c = 2.496$
M5	60.5	152.0	$a = 7.533, b = 5.003, c = 2.548$
M6	75.3	128.0	$a = 7.355, b = 4.867, c = 2.529$
M7	63.8	140.7	$a = 7.422, b = 4.930, c = 2.527$

The calculated lattice parameters are $a = 7.355\text{--}7.552$ Å, $b = 4.867\text{--}5.018$ Å and $c = 2.493\text{--}2.548$ Å. These values are in good agreement with the reported values for the orthorhombic unit cell structure of polyethylene [65]. The order of the grain size is as follows: HDPE/O-MWCNT < HDPE/P-SWCNT < HDPE/Amide-MWCNT < HDPE/P-NWCNT, HDPE/O-SWCNT < HDPE < HDPE/Amide-SWCNT. The order of crystallinity is as follows: HDPE/P-MWCNT < HDPE < HDPE/Amide-MWCNT < HDPE/HDPE/Amide-SWCNT < HDPE/P-SWCNT < HDPE/O-SWCNT < HDPE/O-MWCNT. The highest crystallinity was for the smallest grain size which can indicate the formation of more crystallinity with a decrease in the grain size.

The two crystalline characteristic peaks (110) and (200) remain unchanged after the incorporation of the CNTs. However, for the prepared nanocomposites sheets, there are distinct changes in the intensities (Figure 8) of the two crystalline characteristic peaks (110) and (200), with O-MWCNTs producing the highest effect and amide-MWCNT showing the lowest effect. These results are in good agreement with the DSC results. There were no characteristic peaks for CNTs, indicating that the CNTs are exfoliated in the HDPE polymer matrix, confirming the SEM results [66].

The increase (11.9%) in HDPE crystallinity upon the addition of O-MWCNT resulted from changing the nucleation type of HDPE from the homogeneous to the heterogeneous nucleating, which led to accelerating the nucleation process and the formation of more crystalline grains [57]. This acceleration in the grain growth explained the decrease in grain size (128 Å) due to the transform structure from coarse grains to fine grains, thus creating more grain boundary. This can be attributed to the fact that the pore size of the melted polymer matrix is determined as the CNTs are embedded in the polymer matrix [57].

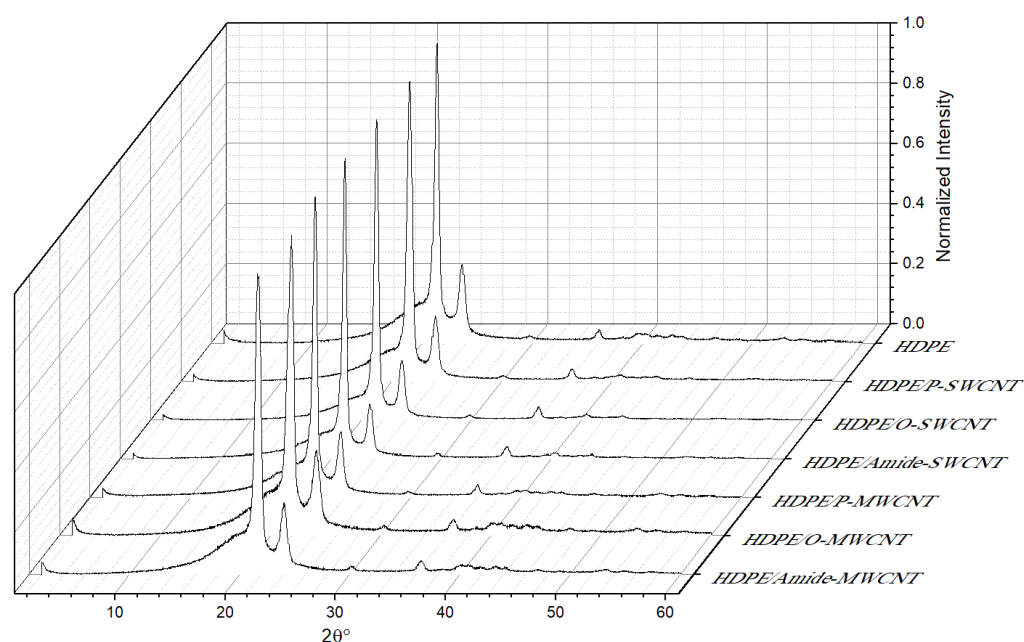


Figure 8. Normalized X-ray diffraction measurements performed on the prepared sheets M1–M7 at 2θ scanning range of $2\text{--}60^\circ$ with a step size of 0.02° .

The presence of an oxygenated functional group at the O-CNTs surface can possess the capability to form a hydrogen bond with the polymer matrix. The increase (4.5%) in HDPE crystallinity upon addition of O-SWCNT compared with O-MWCNT (11.9%) can be attributed to the size difference between O-SWCNT and O-MWCNT, which significantly impacts the crystallinity of the HDPE. The larger size of the O-MWCNT makes the O-MWCNT achieved high interfacial adhesion within the HDPE matrix, which led to the acceleration of the nucleation process and increased crystallization, which is consonant with the DSC results [57,67].

The calculated % crystallinity from the XRD data were in the range 60.5–75.3% which is consistent with the values found in the literature [68]. Although the calculated values of % crystallinity from the DSC data and the XRD values should show the same trend, the calculated values from the DSC data were in the range 28–31%, lower than the calculated values from the XRD, this can be attributed to the previous processing thermal history of the nanocomposite as was explained by Unge et al. [68].

4. Conclusions

Nanocomposite sheets of HDPE and CNTs were prepared by melt compounding methods. Different types of CNTs were used (P-SWCNT, O-SWCNT, amide-SWCNT, P-MWCNT, O-MWCNT, amide-MWCNT) to determine the effects of treatment and type on CNT compatibility with the HDPE polymer. FTIR confirmed the oxidation and functionalization of the prepared CNTs. The thermal stability, crystallinity and crystal structure of the prepared nanocomposites sheets were characterized using TGA, DSC, SEM and X-ray. Additions of MWCNT (pristine and functionalized) to the HDPE matrix showed greater enhancement in thermal stability compared with SWCNT (pristine and functionalized). The maximum enhancement (12°C) was produced by O-MWCNT. This might be explained by the potential for oxidized CNTs to act as radical scavengers, offering improved thermal stability. The addition of pristine or functionalized CNTs to HDPE did not change the crystal structure of the HDPE, but decreased the crystallinity of the polymer, with a maximum decrease caused by the addition of O-SWCNT. Using the melt compounding method to reinforce the HDPE polymer matrix with functionalized MWCNTs, a modified nanocomposite material has been produced which is a candidate for many lightweight, thermally stable applications, and there is a potential to be used as chemical or bio sen-

sors material. Of the produced composites, O-MWCNT showed the best enhancement of thermal properties (12 °C) without affecting the crystallinity or the crystal structure of the HDPE polymer.

Author Contributions: Conceptualization, A.A.B. and R.A.-Z.; methodology, A.B.; formal analysis, R.A.-Z. and A.B.; investigation, A.A.B., A.B. and R.A.-Z.; resources, Y.F.M.; data curation, A.K. and A.B.; writing—original draft preparation, A.B.; writing—review and editing, A.A.B., Y.F.M., R.A.-Z. and A.K.; visualization, R.A.-Z. and Y.F.M.; supervision, A.A.B. and R.A.-Z.; project administration, A.A.B., R.A.-Z. and Y.F.M.; funding acquisition, Y.F.M. and A.A.B. Authorship must be limited to those who have contributed substantially to the work reported. All authors have read and agreed to the published version of the manuscript.

Funding: This research was funded by “King Abdullah II Design and Development Bureau” (KADDB) and the “Deanship of Academic Research (DAR)/The University of Jordan”, Amman, Jordan.

Institutional Review Board Statement: Not applicable.

Informed Consent Statement: Not applicable.

Data Availability Statement: Not applicable.

Conflicts of Interest: The authors declare no conflict of interest.

References

- Gabriel, L.H. History and Physical Chemistry of HDPE, Plastic Pipe Institute. 2011. Available online: <https://www.yumpu.com/en/document/view/10106275/history-and-physical-chemistry-of-hdpe-plastics-pipe-institute> (accessed on 3 March 2018).
- Akay, M. *Introduction to Polymer Science and Technology*; Ventus Publishing Aps.: Eire, Ireland, 2012; ISBN 978-87-403-0087-1.
- Simpson, D.M.; Harrison, I.R. A Study of the Effects of Processing Parameters on the Morphologies and Tensile Modulus of HDPE Blown Films: Application of Composite Theories on a Molecular Level to Characterize Tensile Modulus. *J. Plast. Film Sheeting* **1994**, *10*, 302–324. [[CrossRef](#)]
- High Density Polyethylene (HDPE) Mechanical Properties at 23 °C. Available online: <https://polymerdatabase.com/Commercial%20Polymers/HDPE.html> (accessed on 10 January 2021).
- Jose, J.P.; Joseph, K. Advances in Polymer Composites: Macro- and Microcomposites—State of the Art, New Challenges, and Opportunities. In *Polymer Composites*, 1st ed.; Thomas, S., Kuruvilla, J., Malhotra, S.K., Coda, K., Sreekala, M.S., Eds.; Wiley-VCH Verlag GmbH & Co. KGaA: Weinheim, Germany, 2012; pp. 1–16, ISBN online 9783527645213, print 9783527326242.
- Sahu, A.K.; Sudhakar, K. Effect of UV Exposure on Bimodal HDPE Floats for Floating Solar Application. *J. Mater. Res. Technol.* **2019**, *8*, 147–156. [[CrossRef](#)]
- Wu, S.; Zhang, J.; Xu, X. Studies on High Density Polyethylene (HDPE) Functionalized by Ultraviolet Irradiation and its Application. *Polym. Int.* **2003**, *52*, 1527–1530. [[CrossRef](#)]
- Zhang, X.; Sreekumar, T.V.; Liu, T.; Kumar, S. Properties and Structure of Nitric Acid Oxidized Single Wall Carbon Nanotube Films. *J. Phys. Chem.* **2004**, *108*, 16435–16440. [[CrossRef](#)]
- Tasis, D.; Tagmatarchis, N.; Bianco, A.; Prato, M. Chemistry of Carbon Nanotubes. *Chem. Rev.* **2006**, *106*, 1105–1136. [[CrossRef](#)]
- McCrossan, K.; McClory, C.; Mayoral, B.; Thompson, D.; McConnell, D.; McNally, T.; Murphy, M.; Nicholson, T.; Martin, D.; Halley, P. Composites of Poly(ethyleneterephthalate) Carbon Nanotubes. In *Polymer-Carbon Nanotube Composites Preparation, Properties and Application*, 1st ed.; McNally, T., Potschke, P., Eds.; Woodhead Publishing Limited: Oxford, UK; Cambridge, UK; Philadelphia, PA, USA; New Delhi, India, 2011; pp. 545–586.
- Arash, B.; Wang, Q.; Varadan, V.K. Mechanical Properties of Carbon Nanotubes/Polymer Composites. *Sci. Rep.* **2014**, *4*, 6479. [[CrossRef](#)] [[PubMed](#)]
- Ruoff, R.S.; Qian, D.; Liu, W.K. Mechanical Properties of Carbon Nanotubes: Theoretical Predictions and Experimental Measurements. *CR Phys.* **2003**, *4*, 993–1008. [[CrossRef](#)]
- Zhang, J.; Zou, H.; Qing, Q.; Yang, Y.; Li, Q.; Liu, Z.; Guo, X.; Du, Z. Effect of Chemical Oxidation on the Structure of Single-Walled Carbon Nanotubes. *J. Phys. Chem.* **2003**, *107*, 3712–3718. [[CrossRef](#)]
- Maciejewska, B.M.; Jasiurkowska-Delaporte, M.; Vasylenko, A.I.; Koziot, K.K.; Jurga, S. Experimental and Theoretical Studies on the Mechanism for Chemical Oxidation of Multiwalled Carbon Nanotubes. *RSC Adv.* **2014**, *4*, 28826–28831. [[CrossRef](#)]
- Rosca, I.D.; Watari, F.; Uo, M.; Akasaka, T. Oxidation of Multiwalled Carbon Nanotubes by Nitric acid. *Carbon* **2005**, *43*, 3124–3131. [[CrossRef](#)]
- Datsyuk, V.; Kalyva, M.; Papagelis, K.; Parthenios, J.; Tasis, D.; Siokou, A.; Kallitsis, I.; Galiotis, C. Chemical Oxidation of Multiwalled Carbon Nanotubes. *Carbon* **2008**, *46*, 833–840. [[CrossRef](#)]
- Li, Q.W.; Yan, H.; Ye, Y.C.; Zhang, J.; Liu, Z.F. Defect Location of Individual Single-Walled Carbon Nanotubes with a Thermal Oxidation Strategy. *J. Phys. Chem. Part B* **2002**, *106*, 11085–11088.

18. Osswald, S.; Havel, M.; Gogotsi, Y. Monitoring Oxidation of Multiwalled Carbon Nanotubes by Raman Spectroscopy. *J. Raman Spectrosc.* **2007**, *38*, 728–736. [[CrossRef](#)]
19. Tsang, S.C.; Harris, P.J.F.; Green, M.L.H. Thinning and Opening of Carbon Nanotubes by Oxidation Using Carbon Dioxide. *Nature* **1993**, *362*, 520–522. [[CrossRef](#)]
20. Yang, D.-Q.; Sacher, E. Strongly Enhanced Interaction Between Evaporated Pt Nanoparticles and Functionalized Multiwalled Carbon Nanotubes Via Plasma Surface Modifications: Effects of Physical and Chemical Defects. *J. Phys. Chem. Part C* **2008**, *112*, 4075–4082. [[CrossRef](#)]
21. Zschoerper, N.P.; Katzenmaier, V.; Vohrer, U.; Haupt, M.; Oehr, C.; Hirth, T. Analytical Investigation of the Composition of Plasma-Induced Functional Groups on Carbon Nanotube Sheets. *Carbon* **2009**, *47*, 2174–2185. [[CrossRef](#)]
22. Schonherr, J.; Buchheim, J.; Scholz, P.; Stelter, M. Oxidation of carbon nanotubes with ozone and hydroxyl radicals. *Carbon* **2017**, *111*, 631–640. [[CrossRef](#)]
23. Koh, A.L.; Gidcumb, E.; Zhou, O.; Sinclair, R. Oxidation of Carbon Nanotubes in an Ionizing Environment. *Nano Lett.* **2016**, *16*, 856–863. [[CrossRef](#)]
24. Gromov, A.; Dittmer, S.; Svensson, J.; Nerushev, O.A.; Perez-Garcia, S.A.; Licea-Jimenez, L.; Rychwalski, R.; Campbell, E.E.B. Covalent Amino-functionalisation of Single-Wall Carbon Nanotubes. *J. Mater. Chem.* **2005**, *15*, 3334–3339. [[CrossRef](#)]
25. Li, M.; Boggs, M.; Beebe, T.P.; Huang, C.P. Oxidation of Single-Walled Carbon Nanotubes in Dilute Aqueous Solutions by Ozone as Affected by Ultrasound. *Carbon* **2008**, *46*, 466–475. [[CrossRef](#)]
26. Kuznetsova, A.; Popova, I.; Yates, J.T., Jr.; Bronikowski, M.J.; Huffman, C.B.; Liu, J.; Smalley, R.E.; Hwu, H.H.; Chen, J.G. Oxygen-Containing Functional Groups on Single-Wall Carbon Nanotubes: NEXAFS and Vibrational Spectroscopic Studies. *J. Am. Chem. Soc.* **2001**, *123*, 10699. [[CrossRef](#)]
27. Chiang, Y.; Lin, W.; Chang, Y.C. The influence of Treatment Duration on Multi-Walled Carbon Nanotubes Functionalized by H₂SO₄/HNO₃ Oxidation. *Appl. Surf. Sci.* **2011**, *257*, 2401. [[CrossRef](#)]
28. Rahmat, M.; Hubert, P. Carbon Nanotube-Polymer Interactions in Nanocomposites: A Review. *Compos. Sci. Technol.* **2011**, *72*, 72–84. [[CrossRef](#)]
29. Yang, Y.K.; China, P.R.; XIE, X.L.; China, Y.W.; Mai, Y.W. Functionalization of Carbon Nanotubes for Polymer Nanocomposites. In *Polymer-Carbon Nanotube Composites Preparation, Properties and Application*, 1st ed.; McNally, T., Potschke, P., Eds.; Woodhead Publishing Limited: Oxford, UK; Cambridge, UK; Philadelphia, PA, USA; New Delhi, India, 2011; pp. 55–84.
30. Chen, L.; Xie, H.; Yu, W. Functionalization Methods of Carbon Nanotubes and its Applications. In *Carbon Nanotubes Applications on Electron Devices*, 1st ed.; Marulanda, J., Ed.; Tech Europe, University Campus sTeP Ri: Rijeks, Croatia; Tech China: Shanghai, China, 2011; pp. 213–232.
31. Camargo, P.H.C.; Satyanarayana, K.G.; Wypych, F. Nanocomposites: Synthesis, Structure, Properties and New Application Opportunities. *Mater. Res.* **2009**, *12*, 1–39. [[CrossRef](#)]
32. Moniruzzaman, M.; Winey, K.I. Polymer Nanocomposites Containing Carbon Nanotubes. *Macromolecules* **2006**, *39*, 5194–5205. [[CrossRef](#)]
33. Kasaliwal, G.R.; Villmow, S.P.; Potschke, P. Influence of Material and Processing Parameters on Carbon Nanotube Dispersion in Polymer Melts. In *Polymer-Carbon Nanotube Composites Preparation, Properties and Application*, 1st ed.; McNally, T., Potschke, P., Eds.; Woodhead Publishing Limited: Oxford, UK; Cambridge, UK; Philadelphia, PA, USA; New Delhi, India, 2011; pp. 99–132.
34. Tang, W.; Santare, M.H.; Advani, S.G. Melt Processing and Mechanical Property Characterization of Multi-Walled Carbon Nanotube/High Density polyethylene (MWNT/HDPE) Composite Films. *Carbon* **2003**, *41*, 2279–2785. [[CrossRef](#)]
35. Arora, G.; Pathak, H.; Zafar, S. Fabrication and Characterization of Microwave Cured High-Density Polyethylene/Carbon Nanotube and Polypropylene/Carbon Nanotube Composites. *J. Compos. Mater.* **2019**, *53*, 2091–2104. [[CrossRef](#)]
36. Gao, J.; Shen, Y.; Li, C. Fabrication of High-Density Polyethylene/Multiwalled Carbon Nanotube Composites Via Submerged Friction Stir Processing: Evaluation of Morphological, Mechanical, and Thermal Behavior. *J. Thermoplast. Compos. Mater.* **2017**, *30*, 241–254. [[CrossRef](#)]
37. Ferreira, F.V.; Menezes, B.R.C.; Franceschi, W.; Ferreira, E.V.; Lozano, K.; Cividanes, L.S.; Coutinho, A.R.; Thim, G.P. Influence of Carbon Nanotube Concentration and Sonication Temperature on Mechanical Properties of HDPE/CNT Nanocomposites. *Fuller. Nanotub. Carbon Nanostruct.* **2017**, *25*, 531–539. [[CrossRef](#)]
38. Al-Harhi, M.A.; Bahuleyan, B.K. Mechanical Properties of Polyethylene-Carbon Nanotube Composites Synthesized by In Situ Polymerization Using Metallocene Catalysts. *Adv. Mater. Sci. Eng.* **2018**, *2018*, 4057282. [[CrossRef](#)]
39. Park, C.; Ounaies, Z.; Watson, K.A.; Crooks, R.E.; Smith, J.J.; Lowther, S.E.; Connell, J.W.; Siochi, E.J.; Harrison, J.S.; Clair, T.L.S. Dispersion of Single Wall Carbon Nanotubes by in Situ Polymerization Under Sonication. *Chem. Phys. Lett.* **2002**, *364*, 303–308. [[CrossRef](#)]
40. Spitalsky, Z.; Tasis, D.; Papagelis, K.; Galiotis, C. Carbon Nanotube-Polymer Composites: Chemistry, Processing, Mechanical and Electrical Properties. *Prog. Polym. Sci.* **2010**, *35*, 357–401. [[CrossRef](#)]
41. Sahoo, N.G.; Rana, S.; Cho, J.W.; Li, L.; Chan, S.H. Polymer Nanocomposites Based on Functionalized Carbon Nanotubes. *Prog. Polym. Sci.* **2010**, *35*, 837–867. [[CrossRef](#)]
42. Jagtap, S.B.; Ratna, D. Preparation and Characterization of Rubbery Epoxy/Multiwalled Carbon Nanotubes Composites Using Amino Acid Salt Assisted Dispersion Technique. *Express Polym. Lett.* **2013**, *7*, 329–339. [[CrossRef](#)]

43. Czigany, T.; Deak, T. Preparation and Manufacturing Techniques for Macro- and Microcomposites. In *Polymer Composites*; Thomas, S., Kuruvilla, J., Malhotra, S.K., Goda, K., Sreekala, M.S., Eds.; Wiley-VCH Verlag GmbH & Co. KGaA: Weinheim, Germany, 2012; Volume 1, pp. 111–134.
44. Kanagaraj, S.; Varanda, F.R.; Zhil'tsova, T.V.; Oliveira, M.S.A.; Simoes, J.A.O. Mechanical Properties of High Density Polyethylene/Carbon Nanotube Composites. *Compos. Sci. Technol.* **2007**, *67*, 3071–3077. [\[CrossRef\]](#)
45. Ferreira, F.V.; Francisco, W.; Menezes, B.R.C.; Brito, F.S.; Coutinho, A.S.; Cividanes, L.S.; Coutinho, A.R.; Thim, G.P. Correlation of Surface Treatment, Dispersion and Mechanical Properties of HDPE/CNT Nanocomposites. *Appl. Surf. Sci.* **2016**, *389*, 921–929. [\[CrossRef\]](#)
46. Salehi, S.; Maghmoomi, F.; Sahebani, S.; Zebajad, S.M.; Lazzeri, A. A Study on the Effect of Carbon Nanotube Surface Modification on Mechanical and Thermal Properties of CNT/HDPE Nanocomposite. *J. Thermoplast.* **2019**, *34*, 203–220. [\[CrossRef\]](#)
47. Nobile, M.R.; Somma, E.; Valentino, O.; Simon, G.; Neitzert, H.C. Influence of the Nanotube Oxidation on the Rheological and Electrical Properties of CNT/HDPE Composites. *AIP Conf. Proc.* **2016**, *1736*, 020150. [\[CrossRef\]](#)
48. Zhang, Q.; Rastogi, S.; Chen, D.; Lippits, D. Low Percolation Threshold in Single-Walled Carbon Nanotube/High Density Polyethylene Composites Prepared by Melt Processing Technique. *Carbon* **2006**, *44*, 778–785. [\[CrossRef\]](#)
49. Du, J.; Zhao, L.; Zeng, Y.; Zhang, L.; Li, F.; Liu, P.; Liu, C. Comparison of Electrical Properties between Multi-Walled Carbon Nanotube and Graphene Nanosheet/High Density Polyethylene Composites with a Segregated Network Structure. *Carbon* **2011**, *49*, 1094–1100. [\[CrossRef\]](#)
50. Mohsin, M.E.A.; Arsad, A.; Fouad, H.; Jawaid, M.; Alothman, O.Y. Enhanced Mechanical and Thermal Properties of CNT/HDPE Nanocomposite Using MMT as Secondary Filler, Times of Polymers (TOP) and Composites. *AIP Conf. Proc.* **2014**, *1599*, 206–209. [\[CrossRef\]](#)
51. Azizian, J.; Tahermansouri, H.; Biazar, E.; Heiari, S.; Khoei, D.C. Functionalization of Carboxylated Multiwall Nanotubes with Imidazole Derivatives and Their Toxicity Investigations. *Int. J. Nanomed.* **2010**, *5*, 907–914.
52. Wepasnick, K.A.; Smith, B.A.; Bitter, J.L.; Fairbrother, D.H. Chemical and Structural Characterization of Carbon Nanotube Surfaces. *Anal. Bioanal. Chem.* **2010**, *363*, 1003–1014. [\[CrossRef\]](#) [\[PubMed\]](#)
53. Gillbert, M. *Brydson's Plastics Materials*, 8th ed.; Elsevier (Butterworth-Heinemann): Oxford, UK; Cambridge, MA, USA, 2017.
54. Kodjie, S.L.; Li, L.; Li, B.; Cai, W.; Li, C.Y.; Keating, M. Morphology and Crystallization Behavior of HDPE/CNT Nanocomposite. *J. Macromol. Sci. B Phys.* **2006**, *45*, 231–245. [\[CrossRef\]](#)
55. Shi, X.; Jiang, B.; Wang, J.; Yang, Y. Influence of Wall Number and Surface Functionalization of Carbon Nanotubes on their Antioxidant behavior in highdensity Polyethylene. *Carbon* **2012**, *50*, 1005–1013. [\[CrossRef\]](#)
56. Mohlala, M.S.; Ray, S.S. Preparation and Characterization of Polymer/Multi-Walled Carbon Nanotube Nanocomposites. *Solid State Phenom.* **2008**, *140*, 97–102. [\[CrossRef\]](#)
57. Guo, C.; Sun, F.; Ling, R.; Yao, J.; Zhang, Z.; Zhang, G. Crystallization and Stress Relaxation Behaviors of UHMWPE/CNT Fibers. *J. Vinyl. Addit. Technol.* **2016**, *24*, 229–232. [\[CrossRef\]](#)
58. Li, C.Y.; Li, L.; Cai, W.; Kodjie, S.L.; Tenneti, K.K. Nanohybrid Shish Kebabs: Periodically Functionalized Carbon Nanotubes. *J. Adv. Mater.* **2005**, *17*, 1198–1202. [\[CrossRef\]](#)
59. McNally, T.; Potsch, P.; Halley, P.; Murphy, M.; Martin, D.; Bell, S.E.J.; Brennan, G.P.; Bein, D.; Lemoine, P.; Quinn, J.P. Polyethylene Multiwalled Carbon Nanotube Composites. *Polymer* **2005**, *46*, 8222–8232. [\[CrossRef\]](#)
60. Yang, B.X.; Pramoda, K.P.; Xu, G.Q.; Goh, S.H. Mechanical Reinforcement of Polyethylene Using Polyethylene-Grafted Multi-walled Carbon Nanotubes. *Adv. Funct. Mater.* **2007**, *17*, 2062–2069. [\[CrossRef\]](#)
61. Hulse, S.; Absar, S.; Sultan, Q.N.; Sabet, S.M.; Mahfuz, H.; Khan, M. Synthesis and Characterization of UHMWPE Nanocomposite Fibers Containing Carbon Nanotubes Coated with a PVP Surfactant Layer. *Polym. Compos.* **2018**, *39*, E1025–E1033. [\[CrossRef\]](#)
62. Trujillo, M.; Arnal, M.; Muller, A.; Laredo, E.; Bredeau, D.; Dubis, P. Thermal and Morphological Characterization of Nanocomposites Prepared by in situ Polymerization of High-Density Polyethylene on Carbon Nanotubes. *Macromolecules* **2007**, *40*, 6268–6276. [\[CrossRef\]](#)
63. Chouit, F.; Guellati, O.; Boukhezar, S.; Harat, A.; Guerioune, M.; Badi, N. Synthesis and Characterization of HDPE/N-MWCNT Nanocomposite Films. *Nanoscale Res. Lett.* **2014**, *9*, 288–293. [\[CrossRef\]](#)
64. Speakman, S.A. Introduction to X-ray Powder Diffraction Data Analysis. Material Research Science And Engineering Center. Available online: <https://www.researchgate.net/file.PostFileLoader.html?id=58d22df3dc332d06c7245969&assetKey=AS%3A474618730422273%401490169331513> (accessed on 10 January 2021).
65. TA123, Determination of Polymer Crystallinity by DSC TA Instruments, 109 Lukens Drive, New Castle DE 19720, USA. Available online: <http://www.tainstruments.com/pdf/literature/TA123new.pdf> (accessed on 29 May 2021).
66. Babaei, A.; Ghaffarian, S.R.; Khorasani, M.M.; Abdolrasouli, M.H. Thermal and Mechanical Properties of Ultra High Molecular Weight Polyethylene Fiber Reinforced High-Density Polyethylene Homocomposites: Effect of Processing Condition and Nanoclay Addition. *J. Macromol. Sci. B* **2014**, *53*, 829–847. [\[CrossRef\]](#)
67. Kanai, Y.; Khalap, V.R.; Collins, P.G.; Grossman, J.C. Atomistic Oxidation Mechanism of a Carbon Nanotube in Nitric Acid. *Phys. Rev.* **2010**, *104*, 066401. [\[CrossRef\]](#) [\[PubMed\]](#)
68. Unge, M.; Christen, T.; Tornkuist, C. Electronic structure of Polyethylene crystalline and Amorphous Phases of Pure Polyethylene and their Interfaces. In Proceedings of the 2012 Annual Report Conference on Electrical Insulation and Dielectric Phenomena (CEIDP), Montreal, QC, Canada, 14–17 October 2012. [\[CrossRef\]](#)

Short Biography of Authors

Prof. Abeer Al Bawab Professor of Physical Chemistry in the University of Jordan (UJ) with almost of 24 years teaching experience & specific work interest in enhancing education & conducting research & managing scientific projects (National and International) more than 30 projects with total budget around 3 million JD. Published more than 75 high quality papers in high standard international journals & conferences. Supervisor More than 30 graduate students during her career. Former; General Director of Scientific Research Support Fund (SRF), Ministry of Higher Education & Scientific Research, Jordan, Dean of Academic Research in UJ & Director for a research center (HMCSR) in UJ. Advisor and Scientific Manager for establishing Research Groups through projects & with Young Researchers, Graduate & Undergraduate Students. Abeer Al Bawab is the corresponding author and can be contacted at: drabeer@ju.edu.jo

Dr. Rund Abu-Zurayk Obtained her PhD in Mechanical Engineering from Queen's University Belfast (UK). She obtained her BSc and MSc in Chemical Engineering from the University of Jordan. She is currently the Director of Nanotechnology Center, and an Associate Researcher of Materials Engineering at Hamdi Mango Center for Scientific Research (HMCSR) at the University of Jordan. Research areas are: Water and wastewater treatment; Processing, and applications of polymer nanocomposites in environmental research. She is an author/coauthor of more than 20 papers published in international journals or proceedings of international conferences. She can be contacted at: r.abuzurayk@ju.edu.jo

Dr. Yahia Makableh Has earned his PhD degree in Electrical Engineering from the University of Arkansas in 2015. Currently he is an assistant professor and the supervisor of the central labs in the Institute of Nanotechnology at Jordan University of Science and Technology. His research is focused on investigating Nobel optical Nanomaterials for high efficiency solar cells and energy harvesting. He also works on self-cleaning surfaces and lightweight and high strength Nano-composites. He has published several papers in the field of solar cells and optical Nanomaterials. He was the president of the material research society local chapter at the University of Arkansas. He served before as re-search scientist at King Abdullah II Design and Development Bureau (KADDB) in Jordan. He can be contacted at: yfmakableh@just.edu.jo

Ayat Bozeyya Holds a PhD degree in Physical Chemistry from The University of Jordan (2019). MSc degree in Chemistry (2008) from The University of Jordan, and a BSc degree in Chemistry (2001) from The University of Jordan. Currently, she is an Assistant Professor at the Institute of Nanotechnology at Jordan University of Science and Technology (JORDAN). Her research field is in colloid and surface chemistry; water treatment; polymer nanocomposite preparation and characterization. She is author or coauthors of approximately 30 scientific papers published on international Journals. Adding to that, as a researcher, she was and still involved in many research projects that are funded institutionally, governmentally, and internationally. She can be contacted at: aabouzieh@just.edu.jo

Aya Khalaf Obtained her Master degree in physical chemistry from the University of Jordan. She obtained her BSc in chemistry from the University of Jordan. She is currently Lecturer in Department of Basic Sciences, Faculty of Arts and Science at Al-Ahliyya Amman University. Research areas are: Water and wastewater treatment and photocatalysis nanoparticle. She is coauthor of 2 papers published in international journals. She can be contacted at: a.khaled@ammanu.edu.jo